

Measuring molecular frequencies in the 1–10 μm range at 11-digits accuracy

G. Inero^{1,2}, S. Borri^{1,2}, D. Calonico³, P. Cancio Pastor¹, C. Clivati³, D.

D'Ambrosio¹, P. De Natale^{1,2}, M. Inguscio¹, F. Levi³, and G. Santambrogio^{1,2,3*}

¹*Istituto Nazionale di Ottica-CNR & European Laboratory for Non-Linear Spectroscopy LENS,
Via Nello Carrara 1, 50019 Sesto Fiorentino, Italy*

²*Istituto Nazionale di Fisica Nucleare INFN, Sez. di Firenze, Via Sansone 1, 50019 Sesto Fiorentino, Italy*

³*Istituto Nazionale di Ricerca Metrologica INRIM, Strada delle Cacce 91, 10135 Torino, Italy*

Mid infrared (MIR) photonics is a key region for molecular physics [1]. High-resolution spectroscopy in the 1–10 μm region, though, has never been fully tackled for the lack of widely-tunable and practical light sources. Indeed, all solutions proposed thus far suffer from at least one of three issues: they are feasible only in a narrow spectral range; the power available for spectroscopy is limited; the frequency accuracy is poor. Here, we present a setup for high-resolution spectroscopy that can be applied in the whole 1–10 μm range by combining the power of quantum cascade lasers (QCLs) and the accuracy achievable by difference frequency generation using an OP-GaP crystal. The frequency is measured against a primary frequency standard using the Italian metrological fibre link network. We demonstrate the performance of the setup by measuring a vibrational transition in a highly-excited metastable state of CO around 6 μm with 11 digits of precision, four orders of magnitude better than the value available in the literature [2].

Whereas the fractional accuracy on spectroscopic measurements on atoms has reached the few parts in 10^{18} [3], experiments on molecules perform worse by more than three orders of magnitude. This is due to the richer internal structure of molecules that makes cooling and detection more complicated than in atoms. However, the internal structure and symmetry of molecules, and their strong intramolecular fields can enable totally new measurements. Recent experiments on ThO yielded the most sensitive measurement to date of the electron electric dipole moment [4]. The upper limit found in the 10^{-29} e cm range constrains T-violating physics at the TeV energy scale, comparable to the energy scales explored directly at the Large Hadron Collider. In other experiments, the laboratory assessments of the variation of fundamental constants based on molecular spectroscopy [5, 6] achieve a level of sensitivity similar to astronomical observations looking back in time several billion years. Further experiments are probing energy differences in enantiomers of chiral species [7], testing quantum electrodynamics [8], and searching for a fifth force [9].

The MIR is a natural spectral region for high-resolution spectroscopic studies on molecules because it coincides with fundamental rovibrational transitions, which have strong line strengths and Hz-level natural linewidths. A combination of a cold molecular sample and state-of-the-art photonics in the MIR is the key ingredient to catch up with the atomic physics level of precision.

Since 2014, the development of cold molecules technology has accelerated. First, SrF was trapped in a three-dimensional magneto-optical trap [10]. In the meanwhile, laser cooling of YO [11] and CaF [12], and optoelectrical

cooling of formaldehyde [13] has been reported, achieving temperatures as low as 0.5 mK at 10^{7-8} molecules/cm³ densities [14]. Very recently, an ammonia fountain enabling, in principle, sub-Hz linewidths has been demonstrated [15], as well as laser cooling of CaF below the Doppler limit, to 50 μK [16].

On the other hand, photonics in the MIR remains challenging. Coherent sources must feature sufficient intensity, very narrow linewidths, high frequency stability, and an absolute frequency traceability against the primary frequency standard. Continuous wave (CW) optical parametric oscillators (OPOs) can match these requirements only below 5 μm wavelengths at the price of a difficult operability [17], while difference frequency generation (DFG) process suffers from low emitted powers. In the whole 1–10 μm range, orientation-patterned (OP) GaP provides a reasonable efficiency [18]. Room-temperature QCLs cover the whole 3–25 μm range and feature mW-to-W power levels [19]. They have very narrow intrinsic linewidths [20] although current noise can be very detrimental [21]. However, proper control has yielded linewidths of several hundreds of Hz [22, 23]. Transfer of the accuracy of the microwave frequency standard to the MIR has been achieved by non-linear frequency conversion, leaving only low powers to spectroscopic applications [24–26]. In addition, since the overall accuracy of the RF-MIR bridging by optical frequency combs (OFCs) critically depends on the stability of the OFC repetition rate, a step-change was recently determined by the rise of frequency dissemination by optical fibres [27]. Indeed, RF oscillators disciplined by the Global Positioning System (GPS) can achieve 10^{-14} stability and accuracy only after tens of thousands seconds integration times. Instead, optical transfer of the metrological performances of the primary standard allows to stabilize a near-infrared (NIR) OFC at least at the 10^{-14} level in 1 s, and to achieve the intrinsic uncertainty of the disseminated clock with short interaction times [27].

* santambrogio@lens.unifi.it

All this impressive progress, however, has yet failed to trigger significant breakthroughs in molecular physics, in particular in the 5–10 μm region. Indeed, only isolated high-precision measurements below 5 μm [26] and around 10 μm [5, 25] have been reported.

We developed a laser technology that is suitable for the whole MIR range between 1 and 10 μm with unprecedented metrological features. We demonstrate its performance by measuring a vibrational transition around 6 μm on a highly-excited, metastable state in carbon monoxide with kHz-level accuracy. The experiment is done on a molecular beam with a density of about $10^8/\text{cm}^3$, similar to what is currently obtainable in state-of-the-art setups for cold molecules. Our system is based on three pillars.

First, the frequency reference to the primary standard is transferred by an ultrastable laser at 1542 nm sent over the Italian fibre-link network [28]. This network connects several laboratories all over the national territory (details in the Methods Section), being part of a continental metrological network that is currently under construction.

Second, a CW DFG process in an OP-GaP crystal is used to bridge the gap between the NIR and the MIR. OP-GaP is conveniently transparent in the 1–10 μm range and is the most efficient solution to date to produce light at wavelengths above 5 μm when pumping at 1064 nm, where the most powerful, reliable and stable lasers are available. We recently characterized the linear, thermo-optic, and nonlinear properties of this crystal [18].

Third, the MIR radiation is produced by QCLs whose output is almost entirely used for spectroscopy and not for its frequency control.

Figure 1 shows the main features of the metrological chain to control MIR-QCLs. The NIR-MIR frequency gap is bridged by CW DFG in an OP-GaP crystal pumped by two NIR lasers. Both NIR lasers are locked to an OFC whose repetition rate is referenced and stabilized using the fibre link. Finally, the DFG-MIR radiation is used to phase-lock the QCL using a beat note signal in a HgCdTe detector. The pump laser is a Nd:YAG MOPA system at 1064 nm with a linewidth of 1 kHz and a maximal output power of 50 W, while the signal is provided by a diode laser delivering about 30 mW.

The details of the locking chain are described in the Methods section. To characterize the metrological properties of the MIR light, we analyzed the phase-noise power spectral density (PNPSD) of every step of the chain. The measurement of the phase-noise from the optical link is shown in blue in Fig. 2. The pump laser is phase-locked to the closest comb tooth on a bandwidth of 700 Hz. The residual noise of the pump laser at closed phase-lock-loop (PPL1) (green trace in Fig. 2) is estimated to be limited by the comb noise within the PLL1 bandwidth. At higher frequencies, the pump laser features its free-running noise behaviour. The signal laser is phase-locked (PPL2) to the pump laser through a direct digital synthesis (DDS) scheme [29]. Finally, the QCL is phase locked to the

MIR radiation produced in the OP-GaP crystal with a 300-kHz bandwidth PLL3. When the phase-lock chain is operating, the phase noise of the QCL is reduced by more than nine decades at low frequencies and by more than two decades at 30 kHz (black and red traces for free-running and locked, respectively). The DFG phase noise is expected to follow that of the pump laser scaled by a factor $(1 - N_s/N_p)$, according to the DDS locking scheme, since the noise introduced by PPL2 is negligible. A similar consideration applies to PPL3, whose noise (grey trace) is negligible with respect to the DFG phase noise up to few tens of kHz. Hence, we infer that the QCL linewidth is limited by the Nd:YAG laser and that the QCL long term stability and accuracy reflects reliably the performance of the Cs fountain. Finally, we remark that QCL linewidth and jitter at the kHz level can be further improved by referencing the OFC to an ultra-narrow optical-link-disciplined laser around the Nd:YAG frequency.

To prove the versatility of our setup, we measured a vibrational transition on a slow (318 m/s) molecular beam of highly-excited, metastable CO molecules, in a triple resonance experiment. Over 90% of the QCL power can be coupled to the molecular beam, i.e. about 10 mW. For a typical transition dipole moment of 0.05 debye, this power corresponds to a Rabi frequency of some MHz for a beam waist of 1 mm, which are comfortable numbers for many experiments. The metastable $a^3\Pi_1$, $v = 0$, $J = 1$, + state is prepared with a pulsed laser at 206 nm (1 mJ, 150 MHz bandwidth), whereas the molecules are detected via multiphoton resonance-enhanced ionization from the $v = 1$, $J = 1$, - state with a $1 + 1$ process at 283 nm, after the interaction with the MIR light. The experiment runs at 10 Hz. The stability and robustness of this triple resonance setup allows for rapid scans yielding high signal-to-noise ratios. A 25-minutes scan yields a Doppler-broadened absorption profile with a FWHM of 900 kHz, as the one shown in Fig. 3, which is already about two orders of magnitude narrower than the best value reported in the literature (± 90 MHz) [2]. After 9 hours averaging, we could determine the line center of this vibrational transition on the metastable excited state with an uncertainty of 3 kHz as 51399115447 kHz, with an improvement of more than 4 orders of magnitude [2]. The relative uncertainty of 6×10^{-11} is mainly due to systematic effects to which the QCL frequency uncertainty and linewidth contributes with 2×10^{-14} at worst.

We described the accurate frequency traceability from 1 to 10 μm . The range below 3 μm , which is currently not covered by QCLs, is somehow trivial for the availability of various solid state lasers and very efficient nonlinear crystals. Thus, our setup extends high-resolution, accurate frequency measurements to the whole molecular fingerprint region. Frequency dissemination over fibre network allows, for instance, to synchronize of radio telescopes, realizing a thousand-km wide interferometer, whereas synchronization of spectroscopy laboratories allows for simultaneous monitoring of atomic and molec-

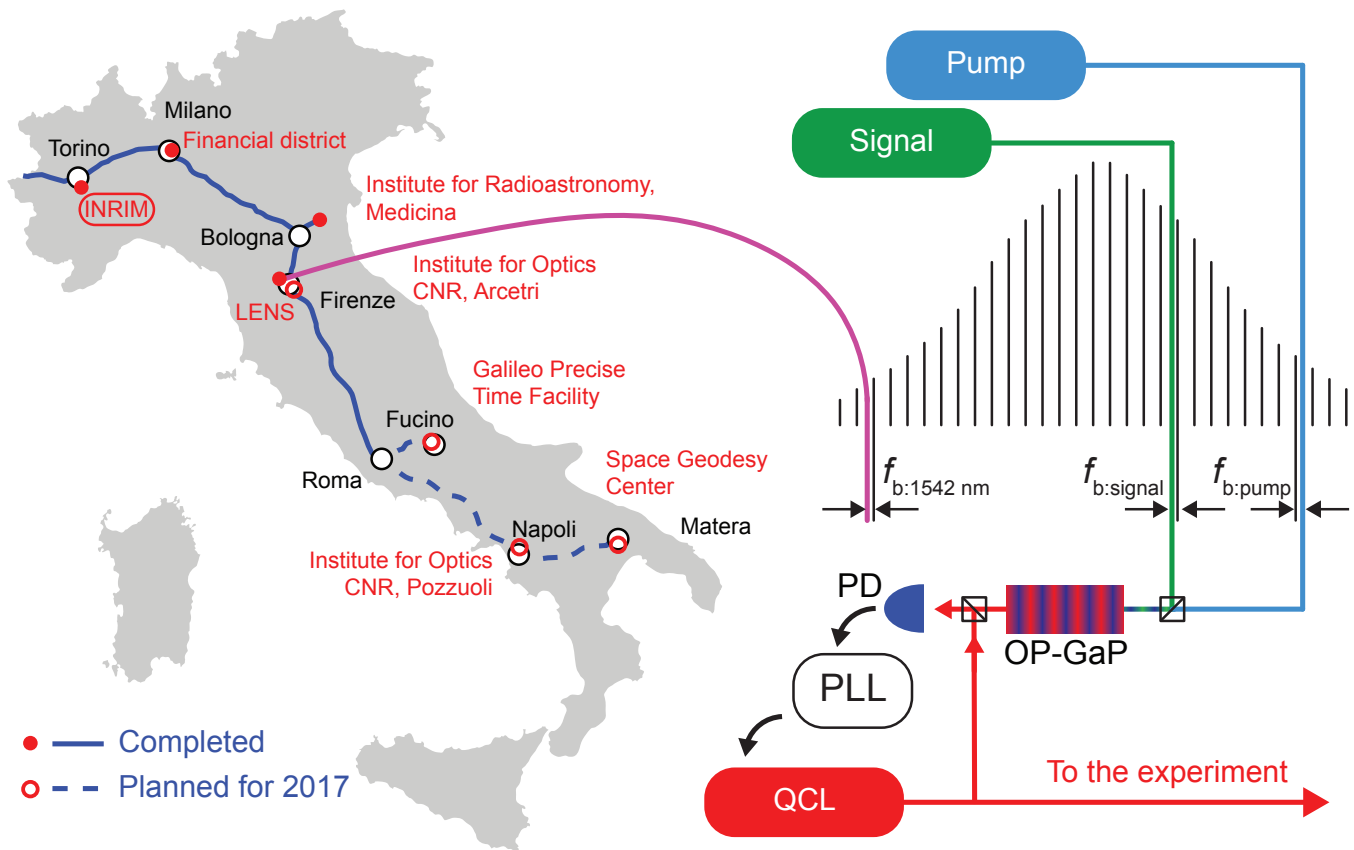


FIG. 1. The left part of the figure shows the Italian fibre link network, blue line, with network nodes in red. At LENS, the ultrastable laser at 1542 nm is used to lock the repetition rate of an OFC. The beat notes of two NIR lasers are measured against the OFC and their frequency difference is kept constant with a direct digital synthesis scheme to cancel out the comb noise contribution. The two lasers are combined in an OP-GaP crystal to generate MIR light, to which a QCL is locked.

ular transitions with unprecedented accuracy that can shed light, for instance, on topological defect dark matter [30]. Moreover, the fibre network together with state-of-the-art MIR photonics and innovative techniques of molecular beam manipulation brings atomic-level accuracies within reach. In particular, the 10^{-16} accuracy allowed by the fibre link can become the standard accuracy for measurements in the MIR ($\sim 10^{13}$ Hz), when molecular cooling techniques will allow for 1-second interaction times. This can disclose new perspectives in fundamental sciences, leading to the replacement of large-scale infrastructures with tabletop setups probing physics at sub-eV energies.

I. METHODS

A. The frequency locking chain

The fibre link network carries the light of an ultrastable laser that is kept at a frequency of $194399996000000.00(4)$ Hz (i.e. around 1542 nm), where the uncertainty is directly related to that of the Cs four-

tain. The laser frequency is referenced to the Italian timescale, generated at the Italian Metrological Institute (INRIM) in Torino. This signal reaches several relevant locations on the national territory: the Institute for Radioastronomy in Medicina (535 km from INRIM), the European Laboratory for Nonlinear Spectroscopy, LENS, in Sesto Fiorentino (642 km), Rome (994 km), and the Italian-French border (150 km). In addition, a timestamp signal referenced to the Italian timescale reaches the financial district in Milano (279 km). During 2017, the fibre network will be extended to the National Institute for Optics INO in Arcetri (662 km), to CNR labs in Pozzuoli (1306 km), to the Galileo Precise Time Facility in Fucino (1134 km), to the Space Geodesy Center in Matera (1684 km), and finally to the French metrological institute LNE-SYRTE in Paris.

A series of bidirectional erbium-doped fibre amplifiers compensate for the almost 200 dB optical losses of the link between INRIM and LENS [28]. The laser at 1542 nm has a stability of 1×10^{-14} at 1 s and an accuracy of 2×10^{-16} ; these performances have been assessed by measuring the absolute frequency of the 1542-nm laser on two independent optical combs referenced to the same

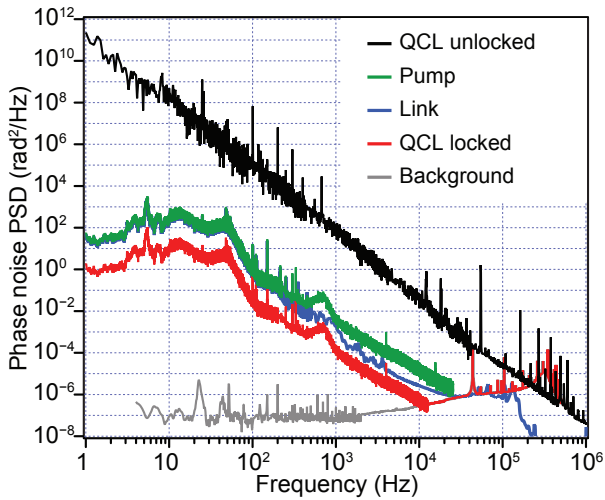


FIG. 2. Phase noise of various components of the frequency locking chain. The phase noise of the free running QCL is shown in black. The noise on the fibre link is shown in blue. The error signal of the phase-lock loop for the pump laser is shown in green. The expected phase noise of the QCL when it is locked to the DFG radiation is shown in red and is obtained by scaling the phase noise of the pump laser, following the virtual beat note scheme.

H-maser. The optical link does not affect the uncertainty of the delivered signal within parts in 10^{19} [28]. However, the signal delivered over the fibre is affected by a large amount of phase noise in the short term (<5 ms) due to the limited bandwidth consequent to the photon round-trip time in the fibre [27].

At LENS a diode laser is phase-locked to the incoming radiation, replicating the stability of the link laser and boosting the optical power at a suitable level for referencing an OFC. The repetition rate f_{rep} of a commercial OFC is then phase-locked to the 1542-nm light using an intra-cavity electro-optic modulator, with a bandwidth of approximately 300 kHz; the lock frequency is properly chosen so that the repetition rate is 100 MHz when the incoming radiation is at the nominal frequency value. The carrier-envelope offset frequency f_0 is stabilized to an RF frequency standard. The phase-noise of the optical comb is then dominated by the residual noise of the stabilized link, which is limited by the fiber length [31].

A Nd:YAG MOPA system at 1064 nm with a linewidth of 1 kHz (pump) and a diode laser at 1301 nm (signal) are locked to the OFC. The beat notes of both lasers to the closest teeth of the OFC are detected with two fast InGaAs photodiodes with a minimum signal-to-noise ratio of 25 dB on a 100 kHz bandwidth. We refer to these beat notes as $f_{\text{b:pump}}$ and $f_{\text{b:signal}}$, and we refer to the absolute frequencies of the two lasers as ν_{pump} and ν_{signal} . Figure 2 shows the phase noise of the beat note $f_{\text{b:pump}}$ between the pump and the closest comb teeth. The link noise is derived from independent measurements [27], and re-scaled to the respective spectral region. The difference frequency $\text{DF} = \nu_{\text{pump}} - \nu_{\text{signal}}$ is stabilized by an indirect

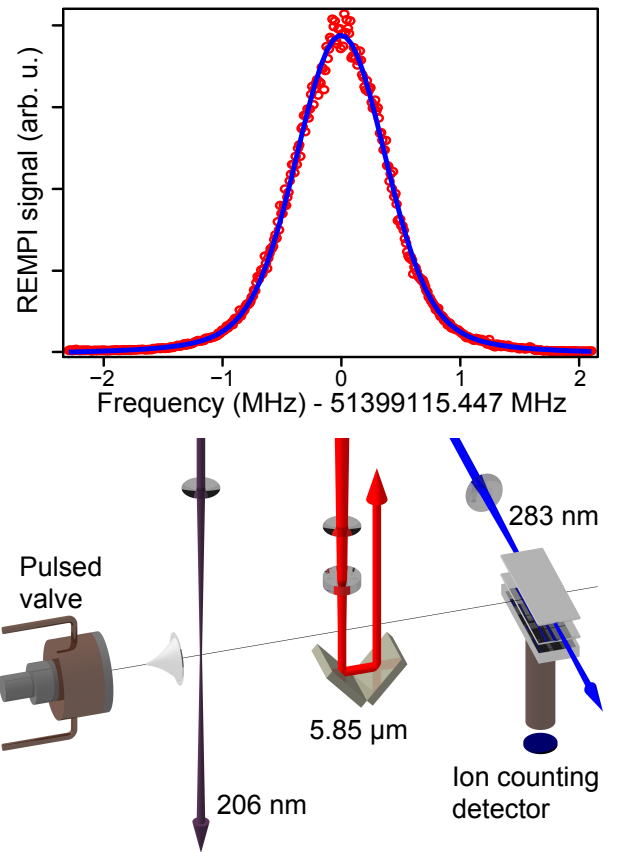


FIG. 3. Top: a typical vibrational absorption spectrum on the $a^3\Pi_1$ metastable state of CO measured in about 20 minutes. The transition $|v=0, J=1, +\rangle \leftarrow |v=1, J=1, -\rangle$ shows a width of 900 kHz. Bottom: sketch of the molecular beam apparatus used for the measurement. The beam is generated by a pulsed valve operated at 10 Hz. CO molecules are skimmed, excited into the metastable state by a UV laser at 206 nm, interact with the mid IR laser, and are finally detected by resonance-enhanced multiphoton ionization. Ions are collected on a microchannel plates detector.

lock of the signal laser to the pump. This is done via the DDS scheme [29], where the OFC bridges the frequency gap between the two lasers but its noise contribution is rejected by proper processing of the $f_{\text{b:pump}}$, $f_{\text{b:signal}}$, and f_0 .

To implement the DDS, f_0 is subtracted from each beat note using analog mixers, to produce $\bar{f}_{\text{b:pump}}$ and $\bar{f}_{\text{b:signal}}$. Thus, the absolute frequencies of the two lasers can be written as $\nu_{\text{pump}} = N_{\text{pump}}f_{\text{rep}} + \bar{f}_{\text{b:pump}}$ and $\nu_{\text{signal}} = N_{\text{signal}}f_{\text{rep}} + \bar{f}_{\text{b:signal}}$, where $N_{\text{pump}} = 2816363$ and $N_{\text{signal}} = 2302371$ are the numbers of the comb's teeth to which the two lasers are beaten. The signal $\bar{f}_{\text{b:signal}} - (N_{\text{signal}}/N_{\text{pump}})\bar{f}_{\text{b:pump}}$ is generated with a 14-bit Direct Digital Synthesizer (DDS) and a mixer, and is stabilized to a RF frequency reference using a PLL which feeds back the signal laser on a bandwidth exceeding 200 kHz. The finite number of digits in the DDS

generates a bias of about 1 Hz in the frequency difference. However, this is calculated and corrected in the final results.

B. Error analysis for the measurement of the vibrational transition

To minimize the systematic Doppler shift due to the imperfect perpendicularity between the MIR laser beam and the molecular beam, the laser light is retro-reflected by a corner cube. Each of the two anti-parallel laser beams induces a Doppler shift on the transition that is equal in magnitude to the other but opposite in sign. Thus, a deviation from the perpendicularity condition manifests itself as a symmetric splitting of the absorption line. The alignment procedure consists in scanning the angle between the laser beam and the molecular beam while recording the magnitude of the splitting; finally, the position of minimal splitting is chosen. The remaining systematic uncertainty is due to imperfect parallelity of the counter-propagating MIR beams. This has been measured and it is better than 10^{-4} rad, which corresponds to a final uncertainty on the transition frequency of 2.6 kHz.

We estimate the Stark and second-order Zeeman shifts due to stray fields to be lower than 10 Hz. As stated

above, we correct for the bias induced by the finite number of digits of the DDS that does not allow to set the perfect value for the DDS. However, the less significant digit of the device introduces a systematic uncertainty that we cannot compensate, which is smaller than 1 Hz. Since the molecular population is first prepared and then detected with focused ns lasers at precisely-known times and positions, we calculate the speed of the molecular beam as 318.5 ± 2 m/s. Thus, the second-order Doppler shift, $+29.4 \pm 0.4$ Hz, is subtracted from the measured frequency. The remaining systematic uncertainty are due to the Cs fountain standard accuracy [32] and to fibre link phase slips [27], both smaller than 100 mHz. Therefore, the *total systematic uncertainty* is estimated as 2.6 kHz.

The Zeeman shift of the $\Delta M = \pm 1$ is of the order of 500 kHz/Gauss, whereas the $\Delta M = 0$ are shifted by about 10 kHz/Gauss. By canceling the Zeeman shift on the $\Delta M = \pm 1$ transitions, we estimate that the residual Zeeman shift on the $\Delta M = 0$ transition is smaller than 1 kHz. This contributes to the statistical uncertainty, together with the uncertainty in the alignment of the beams, whose procedure is described above, and with the fluctuations in the population of metastable CO molecules. The distribution of the experimental measurements has a Gaussian shape with a standard deviation of 7.9 kHz. Our set of 22 scans yields a *total statistical uncertainty* of 1.7 kHz.

-
- [1] S. Borri and G. Santambrogio, *Advances in Physics: X* **1** (2016), 368.
- [2] P. B. Davies and P. A. Martin, *Mol. Phys.* **70** (1990), 89.
- [3] T. L. Nicholson, S. L. Campbell, R. B. Hutson, G. E. Marti, B. J. Bloom, R. L. McNally, W. Zhang, M. D. Barrett, M. S. Safronova, G. F. Strouse, W. L. Tew, and J. Ye, *Nature Comm.* **6** (2015), 6896.
- [4] The ACME Collaboration, J. Baron, W. C. Campbell, D. DeMille, J. M. Doyle, G. Gabrielse, Y. V. Gurevich, P. W. Hess, N. R. Hutzler, E. Kirilov, I. Kozyryev, B. R. O’Leary, C. D. Panda, M. F. Parsons, E. S. Petrik, B. Spaun, A. C. Vutha, and A. D. West, *Science* **343** (2013), 6168.
- [5] A. Shelkownikov, R. J. Butcher, C. Chardonnet, and A. Amy-Klein, *Phys. Rev. Lett.* **100** (2008), 150801.
- [6] S. Truppe, R.J. Hendricks, S.K. Tokunaga, H.J. Lewandowski, M.G. Kozlov, C. Henkel, E.A. Hinds, and M.R. Tarbutt, *Nature Comm.* **4** (2013), 2600.
- [7] B. Darquié, C. Stoeffler, A. Shelkownikov, C. Daussy, A. Amy-Klein, C. Chardonnet, Samia Zrig, L. Guy, J. Crassous, P. Soullard, P. Asselin, T. R. Huet, P. Schwerdtfeger, R. Bast, and T. Saue, *Chirality* **22** (2010), 870.
- [8] E. J. Salumbides, G. D. Dickenson, T. I. Ivanov, and W. Ubachs, *Phys. Rev. Lett.* **107** (2011), 043005.
- [9] E. J. Salumbides, J. C. J. Koelemeij, J. Komasa, K. Pachucki, K. S. E. Eikema, and W. Ubachs, *Phys. Rev. D* **87** (2013), 112008.
- [10] J. F. Barry, D. J. McCarron, E. B. Norrgard, M. H. Steinecker, and D. DeMille, *Nature* **512** (2014), 286.
- [11] M. T. Hummon, M. Yeo, B. K. Stuhl, A. L. Collopy, Y. Xia, and J. Ye, *Phys. Rev. Lett.* **110** (2013), 143001.
- [12] V. Zhelyazkova, A. Cournol, T. E. Wall, A. Matsushima, J. J. Hudson, E. A. Hinds, M. R. Tarbutt, and B. E. Sauer, *Phys. Rev. A* **89** (2014), 053416.
- [13] A. Prehn, M. Ibrügger, R. Glöckner, G. Rempe, and M. Zeppenfeld, *Phys. Rev. Lett.* **116** (2016), 063005.
- [14] E. B. Norrgard, D. J. McCarron, M. H. Steinecker, M. R. Tarbutt, and D. DeMille, *Phys. Rev. Lett.* **116** (2016), 063004.
- [15] C. Cheng, A. P. P. van der Poel, P. Jansen, M. Quintero-Pérez, T. E. Wall, W. Ubachs, and H. L. Bethlem, *Phys. Rev. Lett.* **117** (2016), 253201.
- [16] S. Truppe, H. J. Williams, M. Hambach, L. Caldwell, N. J. Fitch, E. A. Hinds, B. E. Sauer, and M. R. Tarbutt, *arXiv* **1703** (2017), 00580.
- [17] I. Ricciardi, S. Mosca, M. Parisi, P. Maddaloni, L. Santamaria, P. De Natale, and M. De Rosa, *Opt. Lett.* **40** (2015), 4743.
- [18] G. Insero, C. Clivati, D. D’Ambrosio, P. De Natale, G. Santambrogio, P. Schunemann, J.-J. Zondy, and S. Borri, *Opt. Lett.* **41** (2016), 5114.
- [19] M. S. Vitiello, G. Scalari, B. Williams, and P. De Natale, *Opt. Express* **23** (2015), 5167.
- [20] S. Bartalini, S. Borri, P. Cancio, A. Castrillo, I. Galli, G. Giusfredi, D. Mazzotti, L. Gianfrani, and P. De Natale, *Phys. Rev. Lett.* **104** (2010), 083904.
- [21] S. Borri, S. Bartalini, P. Cancio, I. Galli, G. Giusfredi, D. Mazzotti, M. Yamanishi, and P. De Natale, *IEEE J. Quant. Elec.* **47** (2011), 984.
- [22] F. Cappelli, I. Galli, S. Borri, G. Giusfredi, P. Cancio,

- D. Mazzotti, A. Montori, N. Akikusa, M. Yamanishi, S. Bartalini, and P. De Natale, *Opt. Lett.* **37** (2012), 4811.
- [23] M. G. Hansen, E. Magoulakis, Q.-F. Chen, I. Ernsting, and S. Schiller, *Opt. Lett.* **40** (2015), 2289.
- [24] A. Schliesser, N. Picqué, and T. W. Hänsch, *Nature Phot.* **6** (2012), 440.
- [25] B. Argence, B. Chanteau, O. Lopez, D. Nicolodi, M. Abgrall, C. Chardonnet, C. Daussy, B. Darquié, Y. Le Coq, and A. Amy-Klein, *Nature Phot.* **9** (2015), 456.
- [26] I. Galli, M. Siciliani de Cumis, F. Cappelli, S. Bartalini, D. Mazzotti, S. Borri, A. Montori, N. Akikusa, M. Yamanishi, G. Giusfredi, P. Cancio, and P. De Natale, *Appl. Phys. Lett.* **102** (2013), 121117.
- [27] C. Clivati, G. Cappellini, L. F. Livi, F. Poggiali, M. Siciliani de Cumis, M. Mancini, G. Pagano, M. Frittelli, A. Mura, G. A. Costanzo, F. Levi, D. Calonico, L. Fal-lani, J. Catani, and M. Inguscio, *Opt. Express* **24** (2016), 11865.
- [28] D. Calonico, E. K. Bertacco, C. E. Calosso, C. Clivati, G. A. Costanzo, M. Frittelli, A. Godone, A. Mura, N. Poli, D. V. Sutyryn, G. Tino, M. E. Zucco, and F. Levi, *Appl. Phys. B* **117** (2014), 979.
- [29] H.R. Telle, B. Lipphardt, and J. Stenger, *Appl. Phys. B* **74** (2002), 1.
- [30] Y. V. Stadnik and V. V. Flambaum, *Mod. Phys. Lett. A* **29** (2014), 1440007.
- [31] P. A. Williams, W. C. Swann, and N. R. Newbury, *J. Opt. Soc. Am. B* **25** (2008), 1284.
- [32] F. Levi, D. Calonico, C. E. Calosso, A. Godone, S. Micalizio, and G. A. Costanzo, *Metrologia* **51** (2014), 270.

II. ACKNOWLEDGEMENTS

This work was supported by INFN under the SUPREMO project, and by EMPIR-15SIB05-OFTEN, which has received funding from the EMPIR programme co-financed by the Participating States and from the European Union's Horizon 2020 research and innovation programme. The authors gratefully acknowledge P. G. Schunemann and BAE Systems, Inc. for providing the OP-GaP crystal; A. Mura and M. Frittelli for their assistance in the fibre link operation; and M. De Pas for the design and the realisation of the locking electronics at LENS.